

Dynamically-Induced Frustration as a Route to a Quantum Spin Ice State in $\text{Tb}_2\text{Ti}_2\text{O}_7$ via Virtual Crystal Field Excitations and Quantum Many-Body Effects

Hamid R. Molavian,¹ Michel J.P. Gingras,^{1,2} and Benjamin Canals³

¹ *Department of Physics and Astronomy, University of Waterloo, Ontario, Waterloo N2L 3G1, Canada*

² *Department of Physics and Astronomy, University of Canterbury, Private Bag 4800, Christchurch, New Zealand*

³ *Laboratoire Louis Néel, CNRS, BP 166, 38042 Grenoble, France*

(Dated: March 23, 2022)

The $\text{Tb}_2\text{Ti}_2\text{O}_7$ pyrochlore magnetic material is attracting much attention for its *spin liquid* state, failing to develop long range order down to 50 mK despite a Curie-Weiss temperature $\theta_{\text{CW}} \sim -14$ K. In this paper we reinvestigate the theoretical description of this material by considering a quantum model of independent tetrahedra to describe its low temperature properties. The naturally-tuned proximity of this system near a Néel to spin ice phase boundary allows for a resurgence of quantum fluctuation effects that lead to an important renormalization of its effective low energy spin Hamiltonian. As a result, $\text{Tb}_2\text{Ti}_2\text{O}_7$ is argued to be a *quantum spin ice*. We put forward an experimental test of this proposal using neutron scattering on a single crystal.

Magnetic frustration arises when the lattice geometry prevents a system from finding its classical ground state energy by minimizing the energy between pairs of interacting magnetic moments (spins), pair by pair. Particularly interesting are models of geometrically frustrated magnets where there exists a macroscopic number of classical ground states not related by any global symmetry¹. A prominent class of such systems are the *spin ices* where Ising spins reside on a three-dimensional pyrochlore lattice of corner-sharing tetrahedra^{2,3,4}. Because of their macroscopic number of quasi-degenerate low-energy states, spin ice materials possess an extensive low-temperature magnetic entropy^{5,6,7} similar to that found in the proton disordered phase of common water ice⁸.

A current and exciting direction of research in frustrated magnetism is the study of low energy effective Hamiltonians and gauge theories^{9,10,11} to describe highly frustrated systems which, when ignoring quantum effects, display an extensive classical ground state degeneracy similarly to spin ices. Despite the seemingly broad conceptual context of gauge theory approaches, there have so far been few real frustrated quantum magnetic materials identified as potential candidates for the exotic behaviors proposed by these theories¹⁰. In this paper we argue that the paradoxical $\text{Tb}_2\text{Ti}_2\text{O}_7$ (TTO) pyrochlore^{12,13,14,15,16,17,18} belongs to such a class of materials. Specifically, we use a simple model to illustrate that the starting point of the above theories, namely a frustrated Ising spin ice Hamiltonian plus weak transverse terms, indeed constitutes the predominant part of the low energy effective Hamiltonian, H_{eff} , of TTO. However, as we show below, the microscopic mechanism that leads to the “dynamically-induced frustration” and the proposed spin ice assignment for TTO has heretofore escaped scrutiny. We find that frustration and the spin-ice-like structure of H_{eff} dynamically emerge from virtual transitions to excited single-ion crystal field (CF) states and, most importantly, from quantum many-body effects. These transitions drastically modify the symmetries of the many-body wave functions in the low en-

ergy sector, leading to a significant renormalization of the longitudinal (Ising) part of H_{eff} . This renormalization plays a crucial role for materials, such as TTO, that are naturally-tuned near the boundary between a Néel ordered phase and the spin ice states. In particular, these transitions reposition TTO in the spin ice region of coupling parameter space. We are led to suggest that TTO is a novel quantum variant of the classical Ising spin ice materials studied so far^{2,3,4,5,6,7}.

The main reason for the interest devoted to TTO lies in its failure to develop long-range order down to at least 50 mK despite an antiferromagnetic Curie-Weiss temperature, $\theta_{\text{CW}} \sim -14$ K¹³. Similarly to the $\text{Dy}_2\text{Ti}_2\text{O}_7$ (DTO) and $\text{Ho}_2\text{Ti}_2\text{O}_7$ (HTO) spin ices, magnetic Tb^{3+} in TTO possesses a single-ion CF Ising ground state doublet with wavefunctions $|\Psi_0^\pm\rangle$ where $\langle\Psi_0^\pm|J^z|\Psi_0^\pm\rangle$ are the only non-vanishing matrix elements of the \mathbf{J} angular momentum operator^{19,20}. Monte Carlo simulations of a model with such classical Ising spins⁶ that can only point “in” or “out” of an elementary tetrahedron²⁰ and interact via nearest-neighbor (nn) antiferromagnetic exchange^{21,22} and long-range dipolar couplings predict, in dramatic contrast with the experimental findings^{12,14,15,16}, a transition to a four sublattice Néel order at $T_c \sim 1.2$ K⁶. A key difference between TTO and spin ices has so far not been carefully investigated: in spin ices, the excited CF states lie at an energy^{13,19} several hundred times larger than the exchange and dipolar interactions and there is therefore little admixing between the CF states induced by the spin interactions. This is not necessarily the case for TTO where the first excited doublet lies at only $\Delta \sim 18.7$ K above the ground Ising doublet¹³. It is therefore necessary to investigate how the H_{eff} of TTO is affected by virtual quantum mechanical CF excitations.

The Hamiltonian of TTO is taken²¹ as $H = H_{\text{cf}} + H_e + H_d$. H_{cf} is the single-ion CF Hamiltonian¹³, $H_e = \mathcal{J} \sum_{\langle i,j \rangle} \mathbf{J}_i \cdot \mathbf{J}_j$ is the nn exchange interaction and $H_d = \mathcal{D} R_{\text{nn}} \sum_{\langle i,j \rangle} [\mathbf{J}_i \cdot \mathbf{J}_j - 3(\mathbf{J}_i \cdot \hat{r}_{ij})(\mathbf{J}_j \cdot \hat{r}_{ij})] |\mathbf{R}_{ij}|^{-3}$ is the dipole-dipole interaction. $\mathbf{R}_{ij} \equiv \mathbf{R}_j - \mathbf{R}_i = |\mathbf{R}_{ij}| \hat{r}_{ij}$,

where \mathbf{R}_i is the position of atom i with total angular momentum \mathbf{J}_i . \mathcal{J} is the nn exchange coupling with the convention here that $\mathcal{J} > 0$ is antiferromagnetic. $\mathcal{D} = (\mu_0/4\pi)(g\mu_B)^2/R_{\text{nn}}^3$ is the dipolar coupling, and $g = 3/2$ is the Lande factor for Tb^{3+} . $R_{\text{nn}} = 3.59\text{\AA}$ is the nn distance, giving $\mathcal{D} \approx 0.0315\text{ K}$ ¹³. To introduce the single-ion wavefunctions which become admixed by the spin interactions, $H_{\text{int}} = H_e + H_d$, we focus on the essential part of H_{cf} : its doublet ground states, $|\Psi_0^\pm\rangle$, and its lowest excited doublet states, $|\Psi_e^\pm\rangle$, at an energy $\Delta = 18.7\text{ K}$ above $|\Psi_0^\pm\rangle$. The excited states above Δ do not lead to qualitatively different new physics. Tb^{3+} has orbital angular momentum $L=3$, spin $S=3$, and total angular momentum $\mathbf{J} = \mathbf{L} + \mathbf{S}$ with $J=6$. We express $|\Psi_0^\pm\rangle$ and $|\Psi_e^\pm\rangle$ in terms of the eigenstates $|J = 6, m_J\rangle$ of J_z within the fixed $J = 6$ manifold. Exact diagonalization of H_{cf} using the CF parameters taken from Ref. [19] for $\text{Ho}_2\text{Ti}_2\text{O}_7$ but rescaled for $\text{Tb}_2\text{Ti}_2\text{O}_7$ gives: $|\Psi_0^\pm\rangle = \alpha_4|\pm 4\rangle \pm \alpha_5|\mp 5\rangle + \alpha_2|\mp 2\rangle \pm \alpha_1|\pm 1\rangle$ and $|\Psi_e^\pm\rangle = \pm\beta_5|\pm 5\rangle + \beta_4|\pm 4\rangle + \beta_2|\pm 2\rangle \pm \beta_1|\mp 1\rangle$. With $\{\alpha_4, \alpha_5, \alpha_2, \alpha_1\} = (0.9402, -0.2958, 0.1389, 0.0960)$ and $\{\beta_5, \beta_4, \beta_2, \beta_1\} = (0.9271, 0.3117, -0.1917, 0.0809)$.

Exact diagonalization – single tetrahedron. Since the spin correlations in TTO never exceed a length scale much beyond a single tetrahedron¹⁵, we first consider a simple model to describe TTO which consist of non-interacting tetrahedra. Such an approximation of independent tetrahedra explains semi-quantitatively several bulk properties of the classical Heisenberg pyrochlore antiferromagnet model²³. The same approximation also accounts qualitatively well for the spin-spin correlations¹⁵ which, by incorporating transverse spin fluctuations^{22,24}, captures the rough features of the neutron scattering of TTO¹⁵. Our aim in using this approximation is to expose the general effects of virtual CF excitations on H_{eff} . We ignore the long-range dependence of the dipole-dipole interactions in H_{dip} since it is now well understood that it is the nn contribution of the dipolar interactions that predominantly controls the transition from the Néel phase to the spin ice state^{25,26}. Henceforth, we set $\mathcal{D} = 0.0315\text{ K}$ and fix the values of $\{\alpha_m\}$ and $\{\beta_m\}$ to those listed above. We then treat \mathcal{J} and Δ as independent tunable parameters in order to expose the essential physics at play near the Néel – spin ice boundary.

Diagonalizing H_{int} for a single tetrahedron within the space of the $4^4=256$ CF states, we obtain the zero temperature $\mathcal{J} - \Delta$ phase diagram shown in Fig. 1. For the classical Ising limit ($1/\Delta = 0$), we recover the transition between “Néel order” (all-in/all-out, two-fold degenerate, $\mathcal{J} > 5\mathcal{D}$) and a spin ice manifold (two-in/two-out, six fold degenerate, $\mathcal{J} < 5\mathcal{D}$) at $J_{\text{nn}} = D_{\text{nn}}$, where $J_{\text{nn}} \equiv \frac{1}{3}\mathcal{J}|\langle\Psi_0^+|\mathbf{J}^z|\Psi_0^+\rangle|^2$ and $D_{\text{nn}} \equiv \frac{5}{3}\mathcal{D}|\langle\Psi_0^+|\mathbf{J}^z|\Psi_0^+\rangle|^2$ Refs. [6,27]. A classical Ising model^{6,13} places TTO *above* the classical $J_{\text{nn}} = D_{\text{nn}}$ boundary^{6,27} (horizontal dashed line), i.e. in the Néel state¹³. However, for $1/\Delta > 0$, quantum fluctuations, due to the admixing of $|\Psi_0^\pm\rangle$ with $|\Psi_e^\pm\rangle$ via H_{int} , become increasingly important, as shown by the renormalized $\mathcal{J}_c(1/\Delta)$ boundary in Fig. 1 (filled

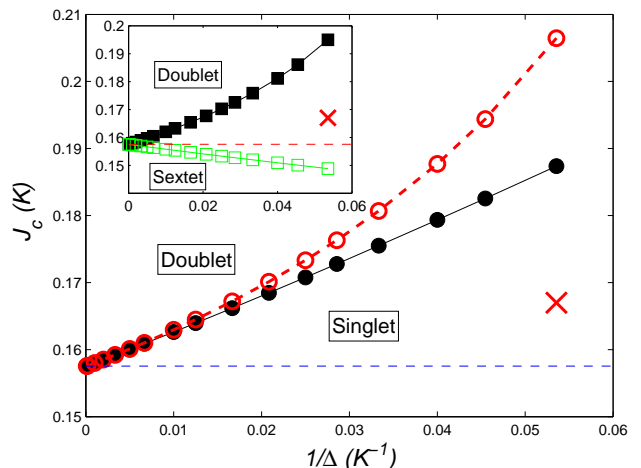


FIG. 1: (Color online). $\mathcal{J} - \Delta$ phase diagram of a single tetrahedron. TTO has $\mathcal{J} = 0.167\text{ K}$ and $\Delta = 18.7\text{ K}$ (cross symbol). Main panel: The boundary $\mathcal{J}_c(1/\Delta)$ (filled circles) separates a ground state singlet ($\mathcal{J} < \mathcal{J}_c$) from a ground state doublet ($\mathcal{J} > \mathcal{J}_c$). The open circles show the same boundary, but as predicted by exact diagonalization of H_{eff} . Inset: neglecting transverse terms in H_{eff} ($\lambda = 0$), the filled squares show the renormalized classical sextet-doublet boundary set by the condition $J_{ij}^{zz}(\mathcal{J}, 1/\Delta) = 0$. The open squares show the *incorrect* sextet-doublet boundary predicted when J_{ij}^{zz} for pair $\langle i, j \rangle$ in H_{eff} is obtained by ignoring contributions in $PHRHP$ coming from (intermediate) excited states $|\Psi_e^\pm\rangle$ that belong to the two other Tb^{3+} ions (k and l) on the tetrahedron.

circles). This boundary separates quantum variants of the classical phases and TTO, with $\mathcal{J} = 0.167\text{ K}$ and $\Delta = 18.7\text{ K}$ (cross symbol in Fig. 1), is now *deeply* repositioned in the singlet regime, i.e. is a *quantum spin ice*. The quantum spin ice state for $\mathcal{J} < \mathcal{J}_c$ is a singlet predominantly built of the fully symmetrized 6 two-in/two-out otherwise degenerate classical spin ice states whose degeneracy is lifted by quantum effects. The ground state also contains a small (of order $1/\Delta$) spectral weight contribution from the excited CF states. The ground singlet is accompanied by a low energy spectrum of 15 excited states that consists of three triplets and three doublets spanning an energy band $\delta W \approx 0.5\text{ K}$ above the ground state, and which is separated by a gap of 16 K from other high energy states. Above the boundary $\mathcal{J}_c(1/\Delta)$, the ground state is an all-in/all-out doublet similarly to the classical $1/\Delta \rightarrow 0$ limit^{3,6}.

Single-tetrahedron model – effective Hamiltonian. To shed light on the virtual CF excitation channels leading to the $\mathcal{J}_c(\Delta)$ above, we construct an effective $S = \frac{1}{2}$ anisotropic Hamiltonian, H_{eff} . Using second order perturbation theory²⁸ in $1/\Delta$, we have $H_{\text{eff}} = PHP + PHRHP$, with $P = \sum_\alpha |\Phi_{0,\alpha}\rangle\langle\Phi_{0,\alpha}|$ and $R = \sum_\beta |\Phi_{e,\beta}\rangle\langle\Phi_{e,\beta}|(E_0 - E_\beta)^{-1}\langle\Phi_{e,\beta}|$, where $E_0 = \langle\Phi_{0,\alpha}|H_{\text{cf}}|\Phi_{0,\alpha}\rangle$ and $E_\beta = \langle\Phi_{e,\beta}|H_{\text{cf}}|\Phi_{e,\beta}\rangle$. Here $\{|\Phi_{0,\alpha}\rangle\}$

are the $2^4 = 16$ states constructed as direct products of the non-interacting single ion $|\Psi_0^\pm\rangle$ CF doublet ground states of H_{cf} . The $|\Phi_{e,\beta}\rangle$ are the remaining $4^4 - 16 = 240$ states. We recast H_{eff} in the form of an effective anisotropic $S = \frac{1}{2}$ spin Hamiltonian in the individual local [111] spin σ_i^z basis²⁰: $H_{\text{eff}} = \sum_{\langle i,j \rangle; \mu, \nu} J_{ij}^{\mu\nu} \sigma_i^\mu \sigma_j^\nu$, where μ, ν are spin component indices, σ_i^μ are Pauli matrices, and $J_{ij}^{\mu\nu}$ are the effective anisotropic coupling constants. A constant energy term has been dropped from H_{eff} , while the one-site $J_i^\mu \sigma_i^\mu$ terms get eliminated by the symmetry of a tetrahedron. Figure 1 shows the singlet-doublet boundary predicted by H_{eff} (open circles).

In order to expose the most important aspects of H_{eff} , we write it as $H_{\text{eff}} = \sum_{\langle i,j \rangle} J_{ij}^{zz} \sigma_i^z \sigma_j^z + \lambda \sum_{\langle i,j \rangle; \mu, \nu} J_{ij}^{\mu\nu} (1 - \delta_{\mu z} \delta_{\nu z}) \sigma_i^\mu \sigma_j^\nu$ with $J_{ij}^{\mu\nu} = J_{ij}^{\mu\nu}(\mathcal{J}, 1/\Delta)$ and with the perturbation parameter λ ultimately set to $\lambda = 1$. H_{eff} contains transverse (non-Ising) $J_{ij}^{\mu\nu} (1 - \delta_{\mu z} \delta_{\nu z}) \sigma_i^\mu \sigma_j^\nu$ terms where, for $\Delta = 18.7$ K, the largest of the transverse $J_{ij}^{\mu\nu}$ is approximately 50% of the Ising J_{ij}^{zz} coupling. To generate these terms via the nonvanishing matrix elements of J_i^z and J_i^\pm between $|\Phi_{0,\alpha}\rangle$ and $|\Phi_{e,\beta}\rangle$ in *PHRHP*, it is important to retain more than the predominant $|\alpha_4| \pm 4\rangle$ and $|\beta_5| \pm 5\rangle$ components in $|\Psi_0^\pm\rangle$ and $|\Psi_e^\pm\rangle$. The term *PHP* corresponds to the classical [111] Ising model with nn exchange and dipolar interactions^{6,13}. It is by accident that \mathcal{J}/\mathcal{D} has a specific value such that *PHP* almost vanishes for TTO^{6,27}, hence allowing an opportunity for the resurgence of quantum effects via *PHRHP* in H_{eff} . The contribution of *PHRHP* to $J_{ij}^{zz} \sigma_i^z \sigma_j^z$ is *ferromagnetic*, and hence competes with the antiferromagnetic classical *PHP* Ising term and brings back frustration in TTO. Neglecting momentarily the quantum transverse terms ($\lambda \rightarrow 0$), the change of sign of $J_{ij}^{zz}(\mathcal{J}, 1/\Delta)$ controls the transition from a (spin ice) two-in/two-out sextet to an all-in/all-out doublet (filled squares in inset of Fig. 1). It is a key point of this paper that it is the renormalization of the Ising sector of the theory, $J_{ij}^{zz}(\mathcal{J}, 0) \rightarrow J_{ij}^{zz}(\mathcal{J}, 1/\Delta)$, caused by virtual CF excitations, that largely determines the $\mathcal{J}_c(1/\Delta)$ boundary (filled circles, main panel) and its upward movement with respect to the classical $J_{ij}^{zz}(\mathcal{J}, 0) = 0$ boundary (horizontal dashed line). Specifically, compare the curve with filled squares in inset of Fig. 1 with the curve with filled circles in the main panel, and note the semi-quantitative agreement.

It is important to note that the virtual excitation of an intervening (third) ion k , with angular momentum \mathbf{J}_k and $H = H_{ik} + H_{kj}$ in *PHRHP*, plays a crucial role in the renormalization of the classical Ising sector $J_{ij}^{zz} \sigma_i^z \sigma_j^z$ for pair $\langle i, j \rangle$ in H_{eff} . Only by including this ‘‘third body’’ contribution do we get the correct trend for the ‘‘classically renormalized’’ $J_{ij}^{zz}(\mathcal{J}, 1/\Delta) = 0$ boundary. Failure to do so gives an incorrect boundary *decreasing* with increasing $1/\Delta$ (curve with open squares in inset of Fig. 1). Hence, it is the quantum many body aspect of the full microscopic quantum $H = H_{\text{cf}} + H_e + H_d$ of TTO that

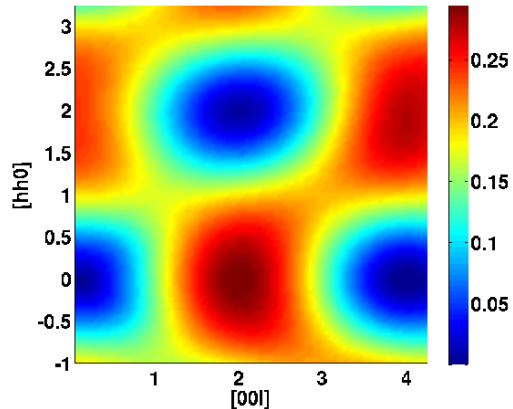


FIG. 2: (Color online) Theoretical diffuse neutron scattering intensity $I(\mathbf{q})/|F(\mathbf{q})|^2$ for a single tetrahedron with four CF states per Tb^{3+} in (hhl) plane at 9 K.

produces the interesting physics here, namely the *correct* renormalization of the Ising part of its H_{eff} from an unfrustrated system when $1/\Delta = 0$ to that of a frustrated ferromagnetic nn spin ice model³. The aforementioned transverse (quantum) part of H_{eff} ($\lambda \neq 0$) lifts the degeneracy of the (classical spin ice) sextet, giving a singlet ground state for an independent tetrahedron and 15 excited states within $\delta W \approx 0.5$ K above the ground state.

Diffuse neutron scattering. The result that H_{eff} for TTO is a nn *ferromagnetic* Ising spin ice model plus transverse terms might come as a surprise and be perceived as incompatible with neutron scattering measurements^{14,15,16}. Indeed, the neutron scattering pattern of TTO^{14,15,16} is qualitatively very different from that of the HTO²⁹ and DTO³⁰ spin ices. In TTO, there is an intensity maximum at 002 in the (hhl) scattering plane and a second broad maximum at 220. In spin ices, there are broad maxima at 003 and $\frac{3}{2}\frac{3}{2}1$ ^{4,29,30}. Therefore, the question is whether the above single tetrahedron model characterized by a ferromagnetic Ising sector in its H_{eff} gives a diffuse neutron scattering pattern compatible with experiment^{14,15,16}. To address this question we compute the diffuse neutron scattering intensity, $I(\mathbf{q})$, using standard formulae³¹: $I(\mathbf{q}) \propto |F(\mathbf{q})|^2 \sum_{a,b;\alpha,\beta} [\delta_{\alpha\beta} - q_\alpha q_\beta / |\mathbf{q}|^2] S_{\text{diff}}^{(a,\alpha;b,\beta)}$ where a, b are the sites on the tetrahedron, α, β are spin components and $F(\mathbf{q})$ is the Tb^{3+} form factor. $S_{\text{diff}}^{(a,\alpha;b,\beta)} = \sum_{n,n'} \langle n | J_a^\alpha | n' \rangle \langle n' | J_b^\beta | n \rangle e^{i\mathbf{q} \cdot (\mathbf{r}_b - \mathbf{r}_a)} e^{-E_n/k_B T}$ where the states $\{n, n'\}$ are those whose energy E_n falls within the experimental energy/frequency resolution window of ~ 4.3 K over which the neutron scattering intensity is energy integrated¹⁵. These are, incidentally, the same low energy states that span an energy $\delta W \approx 0.5$ K above the ground state. Numerical results for $I(\mathbf{q})/|F(\mathbf{q})|^2$ at $T = 9$ K are shown in Fig. 2. One finds a good match in the symmetry of the theoretical pattern in Fig. 2 with the experimental

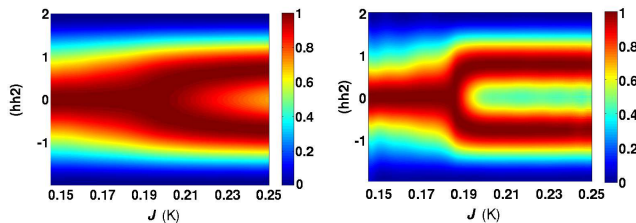


FIG. 3: (Color online) Theoretical diffuse neutron scattering intensity $I(\mathbf{q})/|F(\mathbf{q})|^2$ along $\mathbf{q} = (hh2)$ at 400 mK (left panel) and 40 mK (right panel) as a function of the nearest-neighbor antiferromagnetic exchange \mathcal{J} for a single tetrahedron with four CF states per Tb^{3+} .

one in Fig. 6 of Ref. 15. These results show that, despite a predominant ferromagnetic nn Ising component, H_{eff} possesses sufficient low-energy transverse response (fluctuations) to account for the symmetry of the diffuse neutron scattering. These give, in particular, the intensity maximum at 002 that arise from spin fluctuations transverse to the local [111] Ising directions^{15,22,24}. We propose that a scan of $I(\mathbf{q})/|F(\mathbf{q})|^2$ along the (hh2) direction may be used to ascertain whether TTO is indeed in a quantum spin ice state at low temperatures. Figure 3 shows that $I(\mathbf{q})/|F(\mathbf{q})|^2$ along (hh2) has a broad maximum at $h=0$ in the singlet/spin ice regime, $\mathcal{J} < 0.187$ K for $1/\Delta = 0.053$ K⁻¹ (see main panel, Fig. 1), while it has maxima at $h = \pm\delta(\mathcal{J})$ in the doublet regime for $\mathcal{J} > 0.187$ K. The split hh2 intensity line scan as a characterization of the underlying (antiferromagnet vs spin ice) ground state is sharper the lower the temperature.

Going beyond the single-tetrahedron approximation, competing anisotropic interactions further than nearest neighbors are generated by virtual CF excitations. These lead to a H_{eff} which, at the classical level displays various long-range ordered spin ice states depending on \mathcal{J}/\mathcal{D} . Preliminary calculations find a long-range ordered $\mathbf{Q} = 0$

ferromagnetic (spin ice) state, similar to the one recently reported for $\text{Tb}_2\text{Sn}_2\text{O}_7$ ³², which competes with the previously identified $\mathbf{Q} = 0$ Néel order⁶ and the $\mathbf{Q} = 001$ long range ordered spin ice of the dipolar spin ice model^{25,27}.

In conclusion, we have used a simple model of non-interacting tetrahedra to describe the low temperature properties of the $\text{Tb}_2\text{Ti}_2\text{O}_7$ magnetic pyrochlore material. The present work identifies a new mechanism for dynamically-induced frustration in a physical system which proceeds via crystal field (CF) excitations and quantum many body effects. More specifically, we uncovered that interaction-induced fluctuations among otherwise non-interacting single-ion CF states lead to a renormalization of the low-energy effective theory of $\text{Tb}_2\text{Ti}_2\text{O}_7$ from that of an *unfrustrated* [111] pyrochlore Ising antiferromagnet^{3,6} to a frustrated nearest-neighbor spin ice model^{3,4}. The remaining transverse fluctuations lift the classical ice-like degeneracy and, at the single-tetrahedron level, the system is in a quantum mechanically fluctuating spin ice state, or *resonating spin ice*. The effects discussed here are likely responsible for some of the subtleties underlying the failure of this material to order at a temperature scale of 1 K^{6,13,18,22}. Whether the true quantum mechanical ground state of the full lattice model of $\text{Tb}_2\text{Ti}_2\text{O}_7$ is a semi-classical long-range ordered state with finite quantum spin fluctuations³³, or a more exotic quantum ground state^{9,10,11}, is a challenging but very exciting problem for future studies.

We thank S. Bramwell, S. Curnoe, A. Del Maestro, M. Enjalran, T. Fennell, J. Gardner, B. Gaulin, Y.-J. Kao, S. Rosenkranz, J. Ruff and T. Yavors'kii for very useful discussions. This work was funded by the NSERC of Canada, the Canada Research Chair Program (Tier I, M.G), the Province of Ontario and the Canadian Institute for Advanced Research. M.G. thanks the U. of Canterbury (UC) for an Erskine Fellowship and the hospitality of the Dept. of Physics at UC where part of this work was completed.

¹ R. Moessner, Can. J. Phys. **79**, 1283 (2001).
² M. J. Harris *et al.*, Phys. Rev. Lett. **79**, 255 (1997).
³ S. T. Bramwell and M. J. Harris, J. Phys. Condens. Matter **10**, L215 (1998).
⁴ S. T. Bramwell and M. J. P. Gingras, Science **294**, 1495 (2001).
⁵ A. P. Ramirez *et al.*, Nature **399**, 333 (1999).
⁶ B. C. den Hertog and M. J. P. Gingras, Phys. Rev. Lett. **84**, 3430 (2000).
⁷ A. L. Cornelius and J. S. Gardner, Phys. Rev. B **64**, 060406 (2001).
⁸ L. Pauling, J. Am. Chem. Soc. **58**, 1144 (1936).
⁹ M. Hermele *et al.*, Phys. Rev. B **69**, 064404 (2004).
¹⁰ D. L. Bergman *et al.*, Phys. Rev. Lett. **96**, 097207 (2006).
¹¹ A. H. Castro Neto *et al.*, Phys. Rev. B **74**, 024302 (2006).
¹² J. S. Gardner, *et al.*, Phys. Rev. Lett. **82**, 1012 (1999).
¹³ M. J. P. Gingras *et al.*, Phys. Rev. B **62**, 6496 (2000).

¹⁴ Y. Yasui *et al.*, J. Phys. Soc. Jpn. **71**, 599 (2002); M. Kanada *et al.*, *ibid* **68**, 3902 (1999).
¹⁵ J. S. Gardner *et al.*, Phys. Rev. B **64**, 224416 (2001).
¹⁶ J. S. Gardner *et al.*, Phys. Rev. B **68**, 180401(2003).
¹⁷ K. C. Rule *et al.*, Phys. Rev. Lett. **96**, 177201 (2006); B. G. Ueland *et al.*, *ibid.* **96**, 027216 (2006); A. Keren *et al.*, *ibid.* **92**, 107204 (2004); I. Mirebeau *et al.*, *ibid.* **93**, 187204 (2004); *ibid.*, Nature (London) **420**, 54 (2002).
¹⁸ M. Enjalran *et al.*, J. Phys.: Condens. Matt. **16**, S673 (2004); I. Mirebeau *et al.*, cond-mat/0602384.
¹⁹ S. Rosenkranz *et al.*, J. Appl. Phys. **87**, 5914 (2000).
²⁰ The Ising directions in cubic pyrochlores are local and correspond to the four cubic $\langle 111 \rangle$ directions that intercept elementary tetrahedron unit cells in their middle.
²¹ A random phase approximation (RPA) calculations²² that consider only nn exchange, long-range dipolar couplings and the single-ion CF Hamiltonian of Tb^{3+} describe quan-

- titatively well both elastic and inelastic paramagnetic neutron scattering of TTO¹⁵. Hence, no exceedingly large contribution from either anisotropic electronic exchange, high order electric multipole-multipole interaction, exchange interactions beyond nearest neighbors or virtual phonon exchange is manifestly present in the Hamiltonian H of TTO.
- ²² Y.-J. Kao *et al.*, Phys. Rev. B **68**, 172407 (2003).
- ²³ R. Moessner and A. J. Berlinsky, Phys. Rev. Lett. **83**, 3293 (1999).
- ²⁴ M. Enjalran and M. J. P. Gingras, Phys. Rev. B **70**, 174426 (2004).
- ²⁵ M. J. P. Gingras and B.C. den Hertog, Can. J. Phys. **79**, 1339 (2001).
- ²⁶ S. V. Isakov *et al.*, Phys. Rev. Lett. **95**, 217201 (2005).
- ²⁷ R. G. Melko, *et al.*, Phys. Rev. Lett. **87**, 067203 (2001).
- ²⁸ I. Lindgren and J. Morrison, *Atomic Many-Body Theory, 2nd Edition*, (Springer-Verlag, Berlin [1991]).
- ²⁹ S. T. Bramwell *et al.*, Phys. Rev. Lett. **87**, 047205 (2001).
- ³⁰ T. Fennell *et al.*, Phys. Rev. B **70**, 134408 (2004).
- ³¹ J. Jensen and A. R. Mackintosh, *Rare Earth Magnetism*, (Clarendon Press, Oxford, 1991).
- ³² I. Mirebeau *et al.*, Phys. Rev. Lett. **94**, 246402 (2005).
- ³³ A. G. Del Maestro and M. J. P. Gingras, J. Phys.: Condens. Matter **16**, 3339 (2004).